PROCEEDINGS OF ECOS 2022 - THE 36TH INTERNATIONAL CONFERENCE ON
EFFICIENCY, COST, OPTIMIZATION, SIMULATION AND ENVIRONMENTAL IMPACT OF ENERGY SYSTEMS
25-30 JUNE, 2023, LAS PALMAS DE GRAN CANARIA, SPAIN

Implementation of a semi-empirical model for a low-temperature alkaline electrolyzer in Aspen HYSYS®

Paolo Vitulli[a], Andrea Monforti Ferrario[b,c], Mosè Rossi[c], Gabriele Comodi[c]

[a] Marche Polytechnic University, Department of Information Engineering, Ancona, Italy, p.vitulli@pm.univpm.it
[b] ENEA, Italian National Agency for New Technologies, Energy and Sustainable Economic Development, Rome, Italy, andrea.monfortiferrario@enea.it
[c] Marche Polytechnic University, Department of Industrial Engineering and Mathematical Sciences, Ancona, Italy, a.monforti@pm.univpm.it
[c] Marche Polytechnic University, Department of Industrial Engineering and Mathematical Sciences, Ancona, Italy, mose.rossi@staff.univpm.it, CA
[c] Marche Polytechnic University, Department of Industrial Engineering and Mathematical Sciences, Ancona, Italy, g.comodi@staff.univpm.it

Abstract:
Water electrolysis performed by renewables allows to produce green Hydrogen: this process can boost the penetration of clean energy sources into electric grids. This work presents a model developed in Aspen HYSYS® aiming at evaluating the performance of a low-temperature alkaline (ALK) electrolyzer while varying the main operating conditions (e.g., power supply, temperature, and pressure). A Semi-empirical model published in the scientific literature, which describes the physic-chemical processes at the system level, has been implemented in Aspen HYSYS® and used for resembling the operational behaviour of an ALK electrolyzer. The model consists of common system-level blocks with a customized spreadsheet: semi-empirical correlations, which have been calibrated via multiple non-linear regression fittings of experimental data from the scientific literature, allowed to implement the main electro- and thermochemical-equations of the electrolysis process. Simulated results showed a good agreement with respect to the experimental ones for all the studied operating conditions in terms of Normal Root Mean Square Error (NRMSE). Regarding the Hydrogen flow rate, the comparison between the model and the experimental results showed NRMSE values ranging between $4.208e^{-05}$ and $6.415e^{-05}$, where the former is the lowest threshold value obtained in this analysis. On the other hand, as far as the Hydrogen-to-Oxygen (HTO) is concerned, NRSME values vary between $2.486e^{-04}$ and $5.519e^{-04}$, where the latter is the highest threshold value obtained in this analysis. Finally, this model can be considered a good starting point for creating a Hydrogen-integrated system through the connection of the electrolyzer with a Hydrogen storage system and a fuel cell.

Keywords:
Alkaline electrolyzer, Aspen HYSYS®, Green Hydrogen, Water Electrolysis.

1. Introduction

Nowadays, the need to reduce greenhouse gas emissions, which are the main cause of climate change, is urgently needed as well as having energy systems capable of responding fastly to the increasing energy demands [1]. Current research on the energy sector is focused on the development of technologies capable of exploiting renewable sources in different ways (e.g., direct and indirect) to drastically reduce polluting emissions in the upcoming years.

In such a scenario, Hydrogen seems to be a valid option for easing the ecologic transition; in particular, Water electrolysis through the electricity produced by renewables (green Hydrogen) can provide flexibility to the electric grid, thus increasing the penetration of renewables [2]. Water electrolysis was performed for the first time in 1789 [3] and it consists of three components: the anode, the electrolyte, and the cathode. During the oxidation phase of Hydrogen at the anode, cations reach the cathode via the electrolyte and free electrons flow to the external circuit. Cations and electrons reduce Oxygen to Water at the cathode [4]. Hydrogen produced by Water electrolysis has been thought to be the best energy carrier to counteract the variable nature

https://doi.org/10.52202/069564-0099

of renewables and operate as a middle/long-term energy storage solution in different energy applications [5]. Furthermore, Hydrogen is a non-pollutant molecule since it produces only Water when it undergoes a combustion reaction, thus being considered the cleanest, most efficient, and sustainable fossil fuel alternative [6].

The most known and well-established electrolyzers are alkaline (ALK) and Polymer Exchange Membrane (PEM) ones [7], although the ALK electrolysis is the most reliable in terms of cost and ease of use [8]. The modeling of these electrolyzers is fundamental for simulating and properly resembling the behaviour of Hydrogen-generating systems. Realistic modeling of the overall electrolyzer is important when it is coupled to renewables since it has to correctly face the variable power source; furthermore, it also allows to properly analyse, control, size, manage, and optimize this kind of technology. Besides the technologies previously mentioned regarding the ALK and PEM electrolyzers, this technology is also differentiated by low- and high-temperature operating conditions. Typically, ALK electrolyzers operate at a current density of about 400 mA/cm^2, at moderate temperatures of 70-90 °C, with a cell voltage in the range of 1.85-2.2 V, and conversion efficiencies in the range of 50-70%. ALK electrolyzers do not depend upon a noble metal catalyst for Hydrogen production, and they are easily handled due to the low-temperature operation. The PEM electrolyzer can operate at a current density of 2000 mA/cm^2 at 90 °C and with 2.1 V. The kinetics of Hydrogen and Oxygen production reaction is faster than in ALK electrolyzers due to the acidic nature of the electrolyte and the metal surface of the electrodes. PEM electrolyzers do not use caustic electrolytes as in ALK ones, which might be highly toxic for human beings if a failure occurs. In addition, PEM electrolyzers offer the possibility to use high pressure on the cathode side, while the anode can be operated at atmospheric pressure. When dealing with high-temperature electrolysis, it means that the operating temperature range is above 100°C and Water is in vapor form. This operating condition increases considerably the electrolysis efficiency, but it leads to more complex management of the electrolyzer as well as higher costs due to the use of specific materials. However, technologies like Solid Oxide (SO) electrolyzers are still in development and not yet ready for being commercialized [9]. As for the high-temperature electrolysis, Motazedi et al. [10] examined Hydrogen production from both environmental and economic points of view using Aspen HYSYS® models. Along the same line, JaeHwa et al. [11] developed a SO electrolyzer model in Aspen HYSYS® to perform a sensitivity analysis by varying different operating conditions (e.g., current density, temperature, and pressure).

Moving to ALK electrolyzers, Sánchez et al. [12] have developed a model in Aspen Plus® to resemble the behaviour of the ALK electrolyzer. Nevertheless, to the authors' knowledge, in the scientific literature there are no user-friendly models developed in Aspen HYSYS® related to the ALK Water electrolyzers. The novelty of the present work consists of the development of a user-friendly model related to a low-temperature Water ALK electrolysis stack in the Aspen HYSYS® environment, which is capable of providing the main performance parameters (e.g., electric potential and Hydrogen-to-Oxygen (HTO)) according to different input conditions (e.g., pressure, temperature, current density). As previously said, besides being easily used by end-users, this model can be tailored according to the main specific characteristics of the ALK electrolyzer to be resembled.

The model has been calibrated through regression fitting of semi-empirical process relations and validation with respect to experimental data obtained by [12, 13]. In order to model the stack of the ALK electrolyzer and to carry out the regression of experimental data, the authors based the model development on the analysis carried out by Sánchez et al [13] where a semi-empirical model of the electrochemical behavior of a 15 kW ALK electrolyzer has been proposed. In addition, the work performed by Amores et al. [14] has been used as well because they provided a paradigm for modeling the behaviour of an ALK electrolyzer, modifying the Ulleberg equation [15] with the aim of considering the influence of both temperature and pressure, the electrode/diaphragm distance, and the electrolyte concentration.

The paper is structured as follows: Section 2 presents the methodology used to model the ALK electrolyzer analytically, as well as providing an overview of the Aspen HYSYS® model. Section 3 is devoted to the results obtained by the simulations at different operating conditions in terms of both pressure and temperature, which have been then compared to the experimental results available in the scientific literature by making Normal Root Mean Square Error (NRMSE) comparison. Finally, Section 4 reports the conclusions of the work.

2. Methodology

The models that describe the behaviour of a low-temperature ALK electrolyzer stack with different operating conditions (e.g., current density, temperature, and pressure) typically include the simulation of the following

https://doi.org/10.52202/069564-0099

quantities: i) electric potential, ii) Faraday efficiency, iii) HTO, iv) flow rate of produced Hydrogen, v) electric power absorbed by the stack, vi) thermal power generated by the stack, vii) stack efficiency, and viii) specific consumption. The trend of the last five items is obtained by the first two. In the scientific literature, there are multiple mathematical correlations that describe the same physical phenomenon occurring within the stack. Based on the experimental data obtained by [13], a semi-empirical modeling approach has been chosen and used in this work. The mathematical model used for the stack electric potential is the one proposed by Sánchez et al. [12, 13], which is an improvement of the equation proposed by Ulleberg [15] as reported by Eq. (1).

$$U = U(T,P,i) = U_{rev} + [(r_1 + q_1) + r_2 T + q_2 P] \cdot i + s \cdot \log_{10}\left[\left(t_1 + \frac{t_2}{T} + \frac{t_3}{T^2}\right) \cdot i + 1\right] \quad (1)$$

where U is the cell electric potential, T is the temperature in [°C], P is the pressure in [bar], i is the current density [A/cm^2], and r_i, q_i, and t_i are experimental constants. The total potential U is the sum of the reversible potential U_{rev}, which is given by thermodynamics, the activation, and the ohmic overpotentials related to the kinetic losses of the electrolysis process. It is worth noting that the polarization curve is not investigated in the field of concentration overpotential since it would require a more complex model and experimental data at higher current densities.
The cell reversible potential U_{rev} is a purely thermodynamic quantity and depends on the Gibbs free energy variation ΔG between products and reactants as a function of the operating temperature and pressure as reported by Eq. (2).

$$U_{rev}(T,P) = \frac{\Delta G}{zF} = \frac{\Delta G_{H_2}(T,P) + \frac{1}{2}\Delta G_{O_2}(T,P) - \Delta G_{H_2O}(T,P)}{zF} \quad (2)$$

Regarding Water electrolysis, the reversible cell potential U_{rev}^0 under standard conditions (P^0=1bar, T^0=25°C) is equal to 1.229 V. The value of the reversible voltage is a function of temperature and pressure, thus assuming different values from the standard one as expressed by Eq. (3) that is the Nernst's equation [16]:

$$U_{rev} = U_{rev}^0 + \frac{R \cdot T_K}{z \cdot F} \cdot \ln\left(\frac{p_{H2} \cdot \sqrt{p_{O_2}}}{a_{H_2O}}\right) \quad (3)$$

where T_K is the temperature in [K], R is the universal constant of gases (8.314 J/K mol), z is the number of electrons transferred in the electrolysis reaction (2 mol_{e^-}/mol_{H2}), F is the Faraday constant (96,485 C/mol), a_{H2O} is the coefficient of activity of Water, p_{O2} and p_{H2} are the partial pressure expressed in [bar] of Oxygen and produced Hydrogen, respectively. Assuming that the membrane is subjected to the mechanical equilibrium, the partial pressures of Hydrogen are the same as the Oxygen ones (p_{O2}=p_{H2}=p_{tot}) and, assuming that the coefficient of activity of the Water is approximately equal to 1 [17], Eq. (3) can be written as follows:

$$U_{rev} = U_{rev}^0 + \frac{R \cdot T}{z \cdot F} \cdot \ln\left(P_{tot}^{\frac{3}{2}}\right) \quad (4)$$

The reversible cell potential U_{rev}^0 can be also calculated considering isobaric conditions (at standard pressure P^0 equal to 1 bar) and thus reducing its dependency only on the temperature [17]. In the scientific literature, there are different empirical relationships such as the one proposed by Hammoudi et al. [18] as reported by Eq. (5).

$$U_{rev}^0(T,P^0) = 1.50342 - 9.956 \cdot 10^{-4} T_K + 2.5 \cdot 10^{-7} {T_K}^2 \quad (5)$$

Finally, the reversible potential is calculated by the set of Eq.s (4) and (5). The electrolyzer under investigation consists of 12 cells installed in series; thus, the stack voltage is obtained by multiplying the cell voltage by the number of cells.

https://doi.org/10.52202/069564-0099

$$U_{stack} = N_{cell} \cdot U \quad (6)$$

where N_{cell} is the number of cells installed in series.

The Hydrogen production rate $\dot{n}_{H2}$ [mol/s] is strictly related by the stoichiometry of the reaction and to the applied current *I* [A], which is the same for all the cells connected in series. The Hydrogen production rate is equal to the current density *i* times cell area A_{cell} as reported in Eq. (7) that is the Faraday's equation. As far as the Faraday efficiency η_{Far} is concerned, Sánchez et al. [12, 13] introduced a modification to the η_{Far} Ulleberg's relation [15] with the use of experimental parameters f_{ij} to include also the effect of the temperature as reported by Eq. (8).

$$\dot{n}_{H2} = \eta_{Far} \frac{I}{zF} \quad (7)$$

$$\eta_{Far} = \frac{i^2 \cdot (f_{21} + f_{22} T)}{(f_{11} + f_{12} T) + i^2} \quad (8)$$

As for the HTO, the equation proposed by Hug et al. [19], which describes the HTO dependence on both current density and temperature, has been used by Sánchez et al. [12, 13] and modified by introducing the dependence of pressure as reported by Eq. (9).

$$HTO = C_1 + C_2 T + C_3 T^2 + (C_4 + C_5 T + C_6 T^2) \cdot \exp\left(\frac{C_7 + C_8 T + C_9 T^2}{i}\right) + E_1 + E_2 P + E_3 P^2 + (E_4 + E_5 P + E_6 P^2) \cdot \exp\left(\frac{E_7 + E_8 P + E_9 P^2}{i}\right) \quad (9)$$

where C_1 to C_9 are constants that represent the influence of the temperature in the HTO, and from E_1 to E_9 there are constants that represent the relations between the gas purity and the pressure.

The electrical power absorbed by the stack $\dot{W}_{el}$ allows to evaluate the specific electrical consumption and the stack efficiency as well, as described by Eq. (10).

$$\dot{W}_{el} = U \cdot N_{cell} \cdot i \cdot A_{cell} \quad (10)$$

Regarding the specific consumption c_{sp}, it can be expressed as the ratio between electric power $\dot{W}_{el}$, which is expressed in [kW], and the mass flow rate of the produced Hydrogen $\dot{m}_{H2}$ expressed in [kg/h].

$$c_{sp} = \frac{\dot{W}_{el}}{\dot{m}_{H2}} = \frac{U(i,T,P) \cdot 2F}{10^3 \cdot \eta_F(i,T) \cdot 7.257168} \quad (11)$$

where 7.257168 is a conversion factor in [s•kg/h•mol] that allows to express the molar flow rate of Hydrogen in [kg/h] knowing its value in [mol/s].

Stack electrical efficiency, η_{stack} , is defined as the ratio between the chemical energy contained in the produced hydrogen and the electrical power needed for its production, as shown by Eq. (12).

$$\eta_{stack} = \frac{\dot{n}_{H2} \cdot LHV}{\dot{W}_{el}} \quad (12)$$

where LHV stands for the Lower Heating Value of hydrogen that is equal to 241.82 kJ/mol.

https://doi.org/10.52202/069564-0099

The thermal power $\dot{Q}_{th}$ involved in the electrolysis process, which must be removed to maintain the isothermal condition, is calculated as:

$$\dot{Q}_{th} = i \cdot A_{cell} \cdot (U(i,T,P) - U_{tn}(T,P)) \quad (13)$$

where U_{tn} is the thermoneutral potential of the stack, which is a function of both temperature and pressure.

As previously described, the electrochemical process model is integrated into the Aspen HYSYS® environment using a spreadsheet since the software does not present pre-build blocks for modeling electrochemical components. The rest of the electrolyzer stack (e.g., inlet and outlet fluid management, temperature and pressure settings, etc.) is represented by the common tools made available by the software. Steady-state operations have been considered and the fluid thermodynamic conditions (e.g., pressure and temperature) are set (e.g., isothermal and isobaric conditions are considered for the whole process). The selected *Fluid Package* is the "*Peng-Robinson*". The Water dissociation reaction is defined as a conversion reaction occurring in the "*Electrolysis reactor*", which represents the set of electrodes. Based on the thermodynamic operating conditions (e.g., temperature, pressure) and load current, the reactor sources the main electro- and thermo-chemical equations from the spreadsheet defining the reaction products and the electric power required. U_{rev} is calculated from the thermodynamic fluid property databases, which are embedded in the software, using Eq. (2). The reactor has two material flows at the output: "*Reaction Gas*" and "*Liquid Product*", where the latter is always null since the molar flow rate of the Water entering the model is equal to the molar flow rate of the Hydrogen that is calculated in the spreadsheet using the Faraday equation. The mixture of Hydrogen and Oxygen "*Reaction gas"* is sent to the second component that is the "*Component splitter*" called "*Electrode separator*": through this component it is possible to separate the oxidation and the reduction semi-reactions in the anode and in the cathodic chambers of each cell, respectively. The separator is set up so that the flows are chemically pure at the outputs (no crossover phenomena). The current output flows are corrected with the HTO that is calculated in the spreadsheet: indeed, the amount of Hydrogen separated from the anode flow by the "*Flow splitter",* here called "*Crossover_Tee*", is subsequently mixed to the Oxygen in the anode.

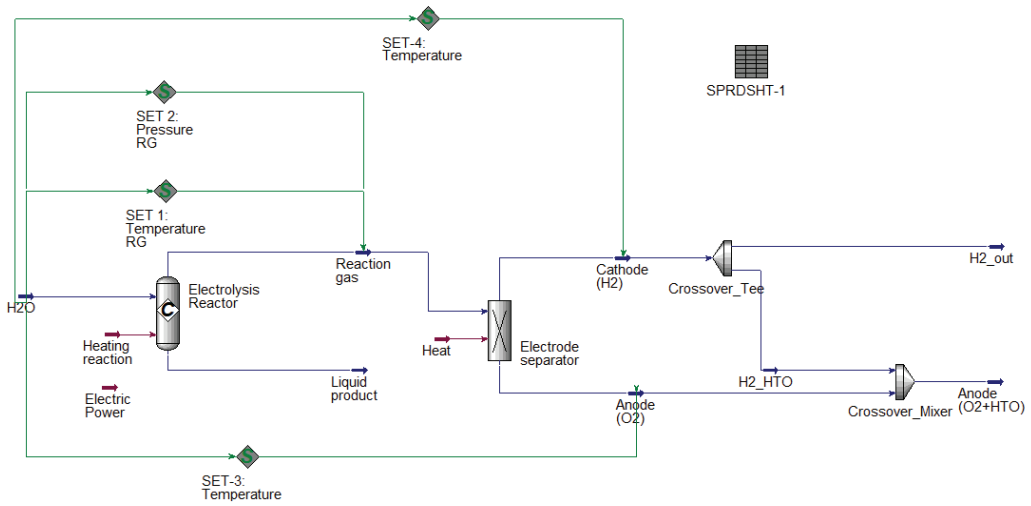

Figure. 1. Model of the low-temperature alkaline electrolyzer developed in Aspen HYSYS®.

In order to obtain comparable simulation results, the electrolyzer that has been modeled is the same one that has been characterized experimentally by Sánchez et al. [12, 13]. It is a small-sized, laboratory scale electrolyzer and its main characteristics are listed in Table 1. To obtain the experimental parameters previously described, the available experimental data have been fitted by using the Matlab® "*Curve Fitting Tool"*. The

https://doi.org/10.52202/069564-0099

regressions are non-linear and multiple, namely two in the case of the Faraday efficiency and three in the case of electric voltage and HTO.

Table 1. Characteristics of the alkaline electrolyzer analysed by Sánchez et al. [12, 13].

Main characteristics	Numerical value	Units of measurement
Hydrogen production flow rate	2.5	m^3/h
Maximum operating pressure	30	bar
Electric potential range	0-120	V
Electric current range	0-500	A
Maximum power	15	kW
The active area of the electrodes	1,000	cm^2
Number of cells	12	-
Electrolyte concentration	30-40	wt% KOH

3. Results and comments

The simulations results, in terms of electrolyzer performance, are evaluated as a function of the current density (between 0-0.5 A/cm^2 with steps of 0.005 A/cm^2) and the parametrization of both pressure and temperature (between 55-85°C with steps of 5°C, and between 1-29 bar with steps of 4 bar). Aspen HYSYS® allows to perform parametric "case studies" and investigate how each variable affects the results while keeping the remained parameters fixed. Figure 2 shows the results related to the stack potential at different values of temperature and pressure. It is worth noting that the trends of the other quantities such as Hydrogen flow rate, etc. have not been here reported.

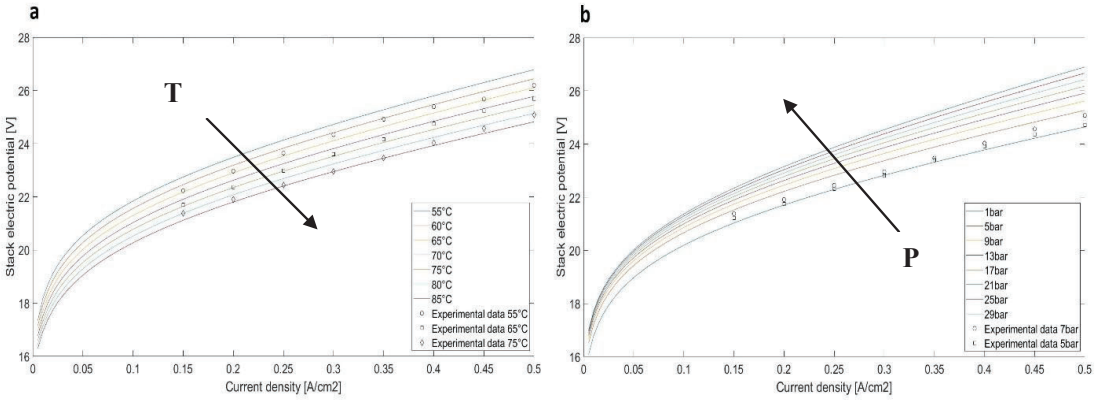

Figure. 2. (a) Stack voltage trend as a function of current density and temperature (pressure equal to 7 bar), and (b) of current density and pressure (temperature equal to 75°C).

In particular, the voltage decreases while the system temperature increases because part of the electric energy required for the electrolysis process is replaced by the associated thermal energy developed during the reaction (see Figure 2). The increase in temperature also improves the reaction kinetics by reducing the activation overpotentials as well as impacting the U_{rev} through the Nernst potential. Furthermore, the electric potential rises when the pressure increases due to the Nernst potential and the one related to the ohmic overpotential.

https://doi.org/10.52202/069564-0099

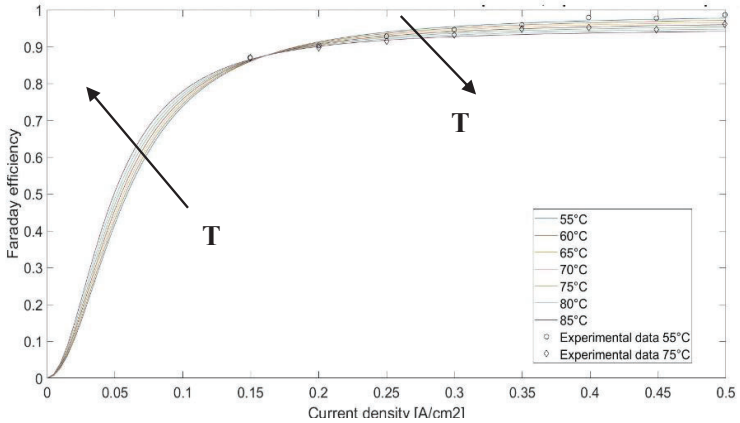

Figure. 3. Faraday efficiency trend as a function of current density and temperature (pressure equal to 7 bar).

Figure 3 shows the trend of the Faraday efficiency as a function of current density and temperature according to Eq. (8). The Faraday efficiency quickly reaches values close to 1 when current density values higher than 0.4 A/cm^2 are used. Conversely, Faraday efficiency decreases when current density values lower than 0.17 A/cm^2 and the increase of temperature leads to lower Faraday efficiency values.

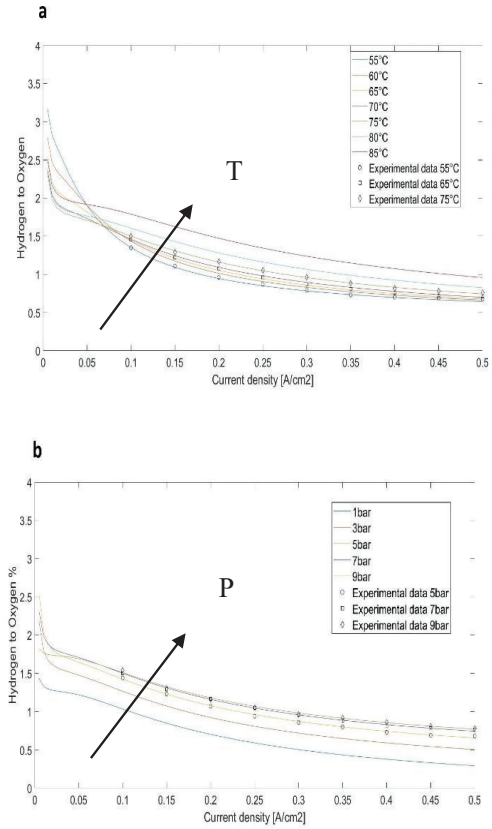

Figure. 4. (a) HTO trend as a function of current density and temperature (pressure equal to 7 bar), and (b) of current density and pressure (temperature equal to 75°C).

https://doi.org/10.52202/069564-0099

Figure 4a shows that the HTO increases when the current density decreases and tends to increase with the increasing temperatures. For this reason, operations with very low values of current density are undesirable because it would be preferable to avoid a HTO beyond the flammability limit of a H_2/O_2 mixture that could lead to combustion or explosion [20]. The higher amount of Hydrogen in the Oxygen stream at higher temperatures is caused by the higher diffusion velocity at elevated temperatures [17]. Figure 4b still shows an increase of the HTO as the current density decreases and as the operating pressure increases. For increasingly small current density values, the HTO model shows an asymptotic behaviour with anomalous variations due to lack of experimental data for very low currents: this means that the model is only valid for the range of density current values for which HTO measurements are available.

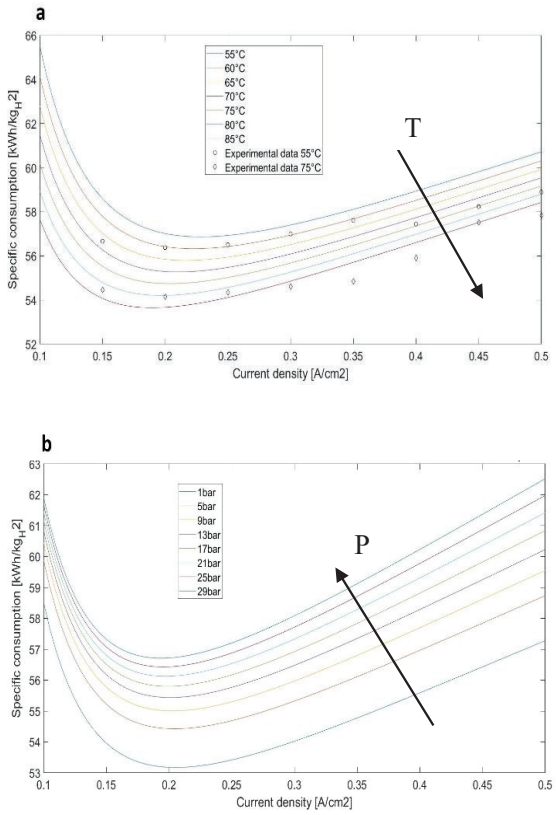

Figure. 5. (a) Specific consumption trend as a function of current density and temperature (pressure equal to 7 bar), and (b) of current density and pressure (temperature equal to 75°C).

Figure 5 shows a non-linear dependence of the specific consumption on the current density. In [13], no experimental data are available for the specific consumption, but these were obtained with data on Faraday efficiency and stack electric potential through Eq. (11). The specific consumption function reaches its minimum value at 0.2 A/cm^2, and it decreases with increasing temperature (see Figure 5a) due to the decrease of the electric potential and increases with the increasing pressure (see Figure 5b) due to the increase of the electric potential. The increase of the specific consumption, when the current density decreases below the threshold of 0.2 A/cm^2, is due to a decrease of the Faraday efficiency that is faster than the electric potential as expressed by Eq. (11). The Faraday efficiency and the electric potential increase with the current density, resulting in an increasing curve for current densities greater than 0.2 A/cm^2. The specific consumption is always between 53 and 63 kWh/kg$_{H2}$.

https://doi.org/10.52202/069564-0099

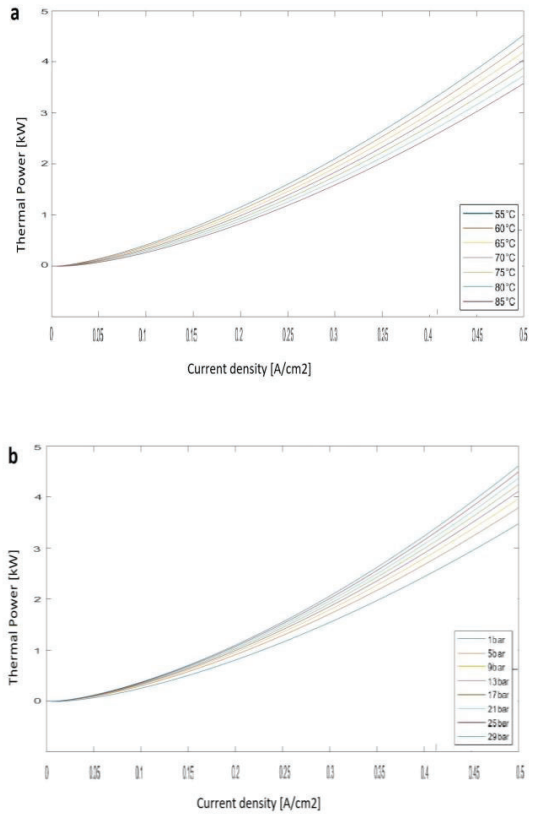

Figure. 6. (a) Thermal power trend as a function of current density and temperature (pressure equal to 7bar), and (b) of current density and pressure (temperature equal to 75°C).

As for the thermal power, Figure 6 shows how it increases with increasing current density and how this trend tends to decrease as the operating temperature increases and to increase as the operating pressure increases. This behaviour can be explained by the influence of both temperature and pressure exert on the stack potential: as the temperature increases the stack potential decreases, while as the pressure increases the potential increases. However, the thermoneutral potential can be considered approximately constant in every case. There are not experimental data for the thermal power. To evaluate the results from the developed model, the *Normal Root Mean Square Error* (NRMSE) has been calculated with respect to the literature experimental values in the same operating conditions reported in [13] (see Table 2).

Table 2. NRMSE values: comparison between model and experimental results.

	7 bar, 55°C	**7 bar, 65°C**	**7 bar, 75°C**	**5 bar, 75°C**	**9 bar, 75°C**
Electric potential	$4.066e^{-04}$	$3.990e^{-04}$	$4.095e^{-04}$	$4.317e^{-04}$	-
Faraday Efficiency	$8.253e^{-05}$	-	$4.871e^{-05}$	-	-
HTO	$5.519e^{-04}$	$2.486e^{-04}$	$3.932e^{-04}$	$4.115e^{-04}$	$3.213e^{-04}$
Specific consumption	$4.859e^{-04}$	-	$4.155e^{-04}$	-	-
Stack efficiency	$4.452e^{-04}$	-	$3.903e^{-04}$	-	-
Electric power	$4.153e^{-04}$	$3.295e^{-04}$	$3.865e^{-04}$	$2.078e^{-05}$	-
Hydrogen flow rate	$6.415e^{-05}$	-	$4.208e^{-05}$	-	-

https://doi.org/10.52202/069564-0099

The regression in Matlab of the cell potential from experimental data was conducted by using the set of Eq.s (4) and (5) where the reversible cell potential U_{rev}^{0} is only a function of the temperature (considering isobaric conditions (at standard pressure P^0 equal to 1 bar) according to [18], while In Aspen HYSYS the reversible cell potential is calculated automatically by implementing Eq. (2). The result is that the numerical value of the reversible cell potential calculated in Aspen HYSYS® is on average greater than the one calculated with the combination of Eq.s. (4) and (5) by 0.0395 V: this is mainly due to the fluid package selected that evaluates the trend of the state function of the components in the system. As a result, an average overestimation of 0.474 V of the electric stack potential of the model developed in Aspen HYSYS® is obtained compared to the experimental data; therefore, also other results are overestimated (e.g., specific consumption and electric power consumed). Conversely, the stack efficiency is underestimated compared to the experimental data. A possible way to increase the accuracy of the model is to perform regressions of the experimental data by firstly calculating the reversible potential according to Eq. (2), and then determining the experimental coefficients from the equation given by the combination of Eq.s. (1) and (2).

4. Conclusions

This work presents and discusses the development of a semi-empirical simulation model developed with Aspen HYSYS® related to a low-temperature Water alkaline electrolysis stack. The main performance parameters (e.g., electric power required and stack efficiency) are evaluated according to different input conditions (e.g., current density, pressure, temperature, etc.).

The trend of the electric potential has been obtained as the sum of the reversible potential and the overpotentials obtained through non-linear multiple regressions performed in Matlab® with the "*Curve Fitting Tool"* of several empirical parameters.

Results show a good agreement with the data made available by the scientific literature (experimental data) for all the analysed quantities within the selected range of operation parameters. Slight differences have been found due to the overestimation of the cell/stack potential related to the electrochemical model: indeed, the comparison between the model and experimental results showed NMRSE values ranging between $3.990e^{-04}$ and $4.317e^{-04}$. Moving to the Faraday efficiency, values ranging between $4.871e^{-05}$ and $8.253e^{-05}$ have been obtained. Then, the specific consumption values varied between $4.155e^{-04}$ and $4.859e^{-04}$, the electric power variation goes from $2.078e^{-05}$ to $4.145e^{-04}$, and the Hydrogen flow rate from $4.208e^{-05}$ to $6.415e^{-05}$ where the former is the lowest threshold value obtained in this analysis. On the other hand, as far as the HTO is concerned, NRSME values vary between $2.486e^{-04}$ and $5.519e^{-04}$, where the latter is the highest threshold value obtained in this analysis. It is worth noting that these results denote that a simple thermodynamic model with the addition of few semi-empirical corrections can represent quite well the operation of the electrolyzer stack without requiring excessive simulation efforts in terms of both kinetic and dynamic behaviours.

The present model will be subsequently implemented in a wider system resembling the behaviour of an integrated Hydrogen system composed by, besides the electrolyzer, a metal hydrides Hydrogen storage and a fuel cell. Furthermore, the future complete model will also take into account both Water recirculation and gas purification processes, which are fundamental in the electrolysis process.

References

[1] EA (2021), Greenhouse Gas Emissions from Energy Data Explorer, IEA, Paris https://www.iea.org/data-and-statistics/data-tools/greenhouse-gas-emissions-from-energy-data-explorer (last accessed 15/05/2023).

[2] IEA (2019), The Future of Hydrogen, IEA, Paris https://www.iea.org/reports/the-future-of-hydrogen, License: CC BY 4.0 (last accessed 15/05/2023).

[3] Jing Zhu, Liangsheng Hu, Pengxiang Zhao, Lawrence Yoon Suk Lee, and Kwok-Yin Wong, Recent Advances in Electrocatalytic Hydrogen Evolution Using Nanoparticles, Chem Rev, Volume 120, 2020, Pages 851-918, https://doi.org/10.1021/acs.chemrev.9b00248.

[4] Lixin Fan, Zhengkai Tu, Siew Hwa Chan, Recent development of hydrogen and fuel cell technologies: A review, Volume 7, 2021, Pages 8421-8446, https://doi.org/10.1016/j.egyr.2021.08.003.

[5] A. Djafour, M. Matoug, H. Bouras, B. Bouchekirma, M.S. Aida, B. Azoui, Photovoltaic-assisted alkaline Water electrolysis: Basic principles, International Journal of Hydrogen Energy, Volume 36, Issue 6, 2011, Pages 4117-4124, https://doi.org/10.1016/j.ijhydene.2010.09.099.

[6] Mingyong Wang, Zhi Wang, Xuzhong Gong, Zhancheng Guo, The intensification technologies to Water electrolysis for hydrogen production – A review, Renewable and Sustainable Energy Reviews, Volume 29, 2014, Pages 573-588, https://doi.org/10.1016/j.rser.2013.08.090.

[7] Z. Abdin, C.J. Webb, E.M. Gray, Modelling and simulation of a proton exchange membrane (PEM) electrolyser cell, International Journal of Hydrogen Energy, Volume 40, Issue 39, 2015, Pages 13243-13257, https://doi.org/10.1016/j.ijhydene.2015.07.129.

[8] Martin David, Carlos Ocampo-Martinez, Ricardo Sanchez-Pena, Advances in alkaline Water electrolyzers: A review, Jounral of Energy Storage, Volume 23, 2019, Pages 392-403, https://doi.org/10.1016/j.est.2019.03.001.

[9] Pierre Millet, Sergey Grigoriev, Chapter 2 – Water Electrolysis Technologies, Renewable Hydrogen Technologies: Production, Purification, Storage, Applications and Safety, 2013, Pages 19-41, https://doi.org/10.1016/B978-0-444-56352-1.00002-7.

[10] Kavan Motazedi, Yaser Khojasteh Salkuyeh, Ian J. Laurenzi, Heather L. MacLean, Joule A. Bergerson, *Economic and environmental competitiveness of high temperature electrolysis for Hydrogen production*, International Journal of Hydrogen Energy, Volume 46, Issue 41, 2021, Pages 21274-21288, ISSN 0360-3199, https://doi.org/10.1016/j.ijhydene.2021.03.226.

[11] JaeHwa KOH, DuckJoo YOON & Chang H. OH (2010) *Simple Electrolyzer Model Development for High-Temperature Electrolysis System Analysis Using Solid Oxide Electrolysis Cell*, Journal of Nuclear Science and Technology, 47:7, 599-607, https://doi.org/10.1080/18811248.2010.9720957.

[12] Mónica Sánchez, Ernesto Amores, David Abad, Lourdes Rodríguez, Carmen Clemente-Jul, *Aspen Plus model of an alkaline electrolysis system for Hydrogen production*, International Journal of Hydrogen Energy, Volume 45, Issue 7, 2020, Pages 3916-3929, ISSN 0360-3199, https://doi.org/10.1016/j.ijhydene.2019.12.027.

[13] Mónica Sánchez, Ernesto Amores, Lourdes Rodríguez, Carmen Clemente-Jul, *Semi-empirical model and experimental validation for the performance evaluation of a 15 kW alkaline Water electrolyzer*, International Journal of Hydrogen Energy, Volume 43, Issue 45, 2018, Pages 20332-20345, ISSN 0360-3199, https://doi.org/10.1016/j.ijhydene.2018.09.029.

[14] Ernesto Amores, Jesús Rodríguez, Christian Carreras*, Influence of operation parameters in the modeling of alkaline Water electrolyzers for hydrogen production*, International Journal of Hydrogen Energy, Volume 39, Issue 25, 2014, Pages 13063-13078, ISSN 0360-3199, https://doi.org/10.1016/j.ijhydene.2014.07.001.

[15] Øystein Ulleberg, *Modeling of advanced alkaline electrolyzers: a system simulation approach*, International Journal of Hydrogen Energy, Volume 28, Issue 1, 2003, Pages 21-33, ISSN 0360-3199, https://doi.org/10.1016/S0360-3199(02)00033-2.

[16] Ernesto Amores, Mónica Sánchez, Nuria Rojas, Margarita Sánchez-Molina, *Renewable hydrogen production by Water electrolysis*, Editor(s): Suman Dutta, Chaudhery Mustansar Hussain, Sustainable Fuel Technologies Handbook, Academic Press, 2021, Pages 271-313, ISBN 9780128229897, https://doi.org/10.1016/B978-0-12-822989-7.00010-X.

[17] Pierre Olivier, Cyril Bourasseau, Pr. Belkacem Bouamama, *Low-temperature electrolysis system modelling: A review*, Renewable and Sustainable Energy Reviews, Volume 78, 2017, Pages 280-300, ISSN 1364-0321, https://doi.org/10.1016/j.rser.2017.03.099.

[18] M. Hammoudi, C. Henao, K. Agbossou, Y. Dubé, M.L. Doumbia, *New multi-physics approach for modelling and design of alkaline electrolyzers*, International Journal of Hydrogen Energy, Volume 37, Issue 19, 2012, Pages 13895-13913, ISSN 0360-3199, https://doi.org/10.1016/j.ijhydene.2012.07.015.

[19] W. Hug, H. Bussmann, A. Brinner, *Intermittent operation and operation modeling of an alkaline electrolyzer*, International Journal of Hydrogen Energy, Volume 18, Issue 12, 1993, Pages 973-977, ISSN 0360-3199, https://doi.org/10.1016/0360-3199(93)90078-O.

[20] H Janssen, J.C Bringmann, B Emonts, V Schroeder, *Safety-related studies on hydrogen production in high-pressure electrolysers*, International Journal of Hydrogen Energy, Volume 29, Issue 7, 2004, Pages 759-770, ISSN 0360-3199, https://doi.org/10.1016/j.ijhydene.2003.08.014.

https://doi.org/10.52202/069564-0099